

Active-IRS-Enabled Target Detection

Xianxin Song, Xiaoqi Qin, Xianghao Yu, Jie Xu, and Derrick Wing Kwan Ng

Abstract—This letter studies an active intelligent reflecting surface (IRS)-enabled non-line-of-sight (NLoS) target detection system, in which an active IRS equipped with active reflecting elements and sensors is strategically deployed to facilitate target detection in the NLoS region of the base station (BS) by processing echo signals through the BS-IRS-target-IRS link. First, we design an optimal detector based on the Neyman-Pearson (NP) theorem and derive the corresponding detection probability. Intriguingly, it is demonstrated that the optimal detector can exploit both the BS’s transmit signal and the active IRS’s reflection noise for more effective detection. Subsequently, we jointly optimize the transmit beamforming at the BS and the reflective beamforming at the active IRS to maximize the detection probability, subject to the maximum transmit power constraint at the BS, as well as the maximum amplification power and gain constraints at the active IRS. Finally, simulation results unveil that the proposed joint beamforming design significantly enhances the detection probability, with the active IRS outperforming its fully- and semi-passive counterparts in detection performance.

Index Terms—Active intelligent reflecting surface (IRS), target detection, joint beamforming optimization.

I. INTRODUCE

Recently, intelligent reflecting surface (IRS) has emerged as a promising technology for future sixth-generation (6G) wireless networks, aiming to enhance both sensing and communication capabilities by dynamically reconfiguring the wireless transmission environment [1]–[3]. Specifically, IRSs can establish additional reflection links from the base station (BS) transceiver to the IRS and then to the sensing target. These links can be leveraged to realize non-line-of-sight (NLoS) target sensing [4] and multi-angle sensing [5], thereby effectively extending the sensing region and enhancing sensing performance in both target detection and estimation.

This letter studies a fundamental IRS-enabled sensing system, in which an IRS is deployed to establish a virtual line-of-sight (LoS) link between the BS and the sensing target, thus realizing NLoS target detection. In such IRS-enabled NLoS target detection system, designing the detector and optimizing the joint beamforming are critical, posing significant challenges due to multiple signal reflections and the intricacies of the coupled variables in the associated non-convex optimization design problem. There are generally three

Xianxin Song and Jie Xu are with the School of Science and Engineering (SSE), the Shenzhen Future Network of Intelligence Institute (FNii-Shenzhen), and the Guangdong Provincial Key Laboratory of Future Networks of Intelligence, The Chinese University of Hong Kong (Shenzhen), Guangdong 518172, China (e-mail: xianxinsong@link.cuhk.edu.cn, xujie@cuhk.edu.cn).

Xiaoqi Qin is with the State Key Laboratory of Networking and Switching Technology, Beijing University of Posts and Telecommunications, Beijing 100876, China (e-mail: xiaoqiqin@bupt.edu.cn).

Xianghao Yu is with the Department of Electrical Engineering, City University of Hong Kong, Hong Kong (e-mail: alex.yu@cityu.edu.hk).

Derrick Wing Kwan Ng is with the School of Electrical Engineering and Telecommunications, University of New South Wales, Sydney, NSW 2052, Australia (e-mail: w.k.ng@unsw.edu.au).

Xianghao Yu and Jie Xu are the corresponding authors.

different types of IRSs applicable for sensing, namely fully-passive IRS, semi-passive IRS, and active IRS. The fully-passive IRS consists of passive reflecting elements that can alter the phase shift of incident signals without introducing any amplification. As a result, the corresponding target sensing is implemented at the BS by processing echo signals through the BS-IRS-target-IRS-BS link [4], [5]. Next, the semi-passive IRS, equipped with dedicated sensors for signal processing, conducts target sensing at the IRS, exploiting echo signals through the BS-IRS-target-IRS link [6], [7]. Furthermore, the active IRS is deployed with active reflecting elements for adaptive signal amplification and phase adjustment along with dedicated sensors. Indeed, the BS-IRS-target reflection link in practice often suffers from distance-product path loss, which significantly restricts sensing performance. Consequently, the active IRS presents great potential to efficiently compensate for this substantive path loss by amplifying the incident signal. In the literature, various prior works [4]–[13] have investigated fully-passive IRS sensing [4], [5], semi-passive IRS sensing [6], [7], and active IRS sensing [8] and ISAC [9]–[13], with a handful of works studying at active-IRS-enabled wireless communications [14], [15]. However, the above prior works about active-IRS-enabled sensing and ISAC adopted target illumination power [9] and beampattern match error [10] as sensing performance metrics, or treated the active IRS’s reflection noise as harmful interference [8], [11]–[13]. Indeed, the potential roles of active IRS’s reflection noise in detection, the optimal detector that exploits both the BS’s transmit signal and the IRS’s reflection noise, and the design of joint beamforming are areas that remain unexplored. These research gaps serve as the motivation for our investigation in this work.

In this letter, we consider target detection enabled by an active IRS, in which the active IRS is deployed to detect the presence of a target by processing echo signals from the BS-IRS-target-IRS link. First, we design an optimal detector based on the Neyman-Pearson (NP) theorem. It is demonstrated that the obtained optimal detector jointly harnesses both the BS’s transmit signal and the active IRS’s reflection noise for effective target detection. Then, we derive the detection probability under a predetermined false alarm probability. Next, we jointly optimize the transmit beamforming at the BS, alongside the phase shift and amplification matrices at the active IRS, to maximize the derived detection probability. This optimization adheres to the maximum transmit power constraint at the BS and the maximum amplification power and gain constraints at the active IRS. Finally, simulation results demonstrate that the proposed joint beamforming design achieves higher detection probability, verifying that the adoption of an active IRS can significantly increase the detection performance compared with fully- and semi-passive counterparts.

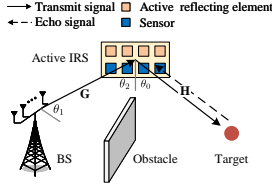


Fig. 1. Illustration of active IRS-enabled target detection.

Notations: Boldface letters refer to vectors (lower case) or matrices (upper case). For a square matrix \mathbf{S} , $\text{tr}(\mathbf{S})$ denotes its trace and $\mathbf{S} \succeq \mathbf{0}$ means that \mathbf{S} is a positive semi-definite matrix. For an arbitrary-size matrix \mathbf{M} , \mathbf{M}^* , \mathbf{M}^T , and \mathbf{M}^H denote its conjugate, transpose, and conjugate transpose, respectively. Let $\mathcal{CN}(\mathbf{0}, \Sigma)$ denote the distribution of a circularly symmetric complex Gaussian (CSCG) random vector with mean vector $\mathbf{0}$ and covariance matrix Σ , and \sim denote “distributed as”. The spaces of $x \times y$ real and complex matrices are denoted by $\mathbb{R}^{x \times y}$ and $\mathbb{C}^{x \times y}$, respectively. Let $\text{diag}(a_1, \dots, a_N)$ denote a diagonal matrix with diagonal elements a_1, \dots, a_N , \otimes denote the Kronecker product, $\|\cdot\|$ denote the Euclidean norm, and $\mathbb{E}(\cdot)$ denote the statistical expectation.

II. SYSTEM MODEL

As shown in Fig. 1, we consider an active IRS-enabled target detection system consisting of one BS with M_t uniform linear array (ULA) transmit antennas, one active IRS with N ULA active reflecting elements and M_r ULA sensors, and one potential target located at the BS’s NLoS region¹. We consider a binary detection task, which aims to decide the presence of a target by processing echo signals from the BS-IRS-target-IRS link. Let hypotheses \mathcal{H}_1 and \mathcal{H}_0 denote the cases when the target is present and absent, respectively.

First, we introduce the channel models. We assume that the BS-IRS and IRS-target-IRS links are dominated by the LoS links [16], [17]. Without loss of generality, we assume that the distance between adjacent transmit antennas at the BS, as well as that between adjacent reflecting elements or sensors at the IRS are all equal to half carrier wavelength. Let vector $\mathbf{e}(\varsigma, K) \in \mathbb{C}^{K \times 1}$ denote the steering vector function of a ULA with size K towards any angle ς , i.e., $\mathbf{e}(\varsigma, K) = [1, e^{j\pi \sin \varsigma}, \dots, e^{j\pi(K-1) \sin \varsigma}]^T$. The angle of the IRS with respect to (w.r.t.) the BS’s transmit antennas and the angle of the BS w.r.t. the IRS’s reflecting elements are denoted as θ_1 and θ_2 , respectively. The distances of the BS-IRS and IRS-target links are denoted as d_1 and d_2 , respectively. As such, the channel matrix of the BS-IRS link is given as $\mathbf{G} = \sqrt{L(d_1)} \mathbf{e}(\theta_2, N) \mathbf{e}^T(\theta_1, M_t) \in \mathbb{C}^{N \times M_t}$, where $L(d_1)$ is the associated channel path loss. Similarly, the target response matrix of the IRS-target-IRS link is modeled as $\mathbf{H} = \alpha \mathbf{e}(\theta_0, M_r) \mathbf{e}^T(\theta_0, N) \in \mathbb{C}^{M_r \times N}$, where $\alpha = \beta L(d_2) \in \mathbb{C}$ is the channel coefficient depending on both the radar cross section (RCS) of the target β and the path loss of the IRS-target link $L(d_2)$ [4], [13], and θ_0 is the angle of target w.r.t. the IRS².

¹This work can be extended to the multi-target case by extending the two hypotheses tests to multiple hypotheses tests.

²In this work, we focus on the target detection at a specified location, based on which the target coefficient α and angle θ_0 can be predicted *a priori*. As such, we assume that α and θ_0 are known to facilitate the analysis.

Next, we present the signal transmission model. We focus on the target detection over a block with a total of T sensing symbols. Let $\mathcal{T} = \{1, \dots, T\}$ denote the set of symbols in the block. The transmit signal by the BS at symbol $t \in \mathcal{T}$ is denoted as $\mathbf{x}(t) \in \mathbb{C}^{M_t \times 1}$ with sample covariance matrix $\mathbf{R}_x = \frac{1}{T} \sum_{t=1}^T \mathbf{x}(t) \mathbf{x}^H(t) \succeq \mathbf{0}$ [4], [6]. Note that the transmit signal $\mathbf{x}(t)$ is deterministic and thus known by the IRS sensors prior to target sensing. Let P denote the maximum BS transmit power, i.e., $\frac{1}{T} \sum_{t=1}^T \|\mathbf{x}(t)\|^2 = \text{tr}(\mathbf{R}_x) \leq P$. Also, the phase shift matrix at the active IRS is denoted as $\Phi = \text{diag}(e^{j\phi_1}, \dots, e^{j\phi_N}) \in \mathbb{C}^{N \times N}$ with $\phi_n \in (0, 2\pi]$, $\forall n \in \mathcal{N}$, and the amplification matrix at the active IRS is denoted as $\mathbf{A} = \text{diag}(a_1, \dots, a_N) \in \mathbb{R}^{N \times N}$ with $0 \leq a_n \leq a_{\max}$, $\forall n \in \mathcal{N}$, where a_{\max} is the maximum amplification gain at each active reflecting element. After the signal transmission from the BS to the IRS and the IRS’s reflection, the departed signal from the active IRS is $\mathbf{A}\Phi\mathbf{G}\mathbf{x}(t) + \mathbf{A}\Phi\mathbf{z}(t)$, where $\mathbf{z}(t) \sim \mathcal{CN}(\mathbf{0}, \sigma_z^2 \mathbf{I}_N)$ is the active IRS’s reflection noise and σ_z^2 is the inherent noise power at each IRS’s reflecting element. Let P_A denote the maximum IRS amplification power, i.e., $\frac{1}{T} \sum_{t=1}^T \|\mathbf{A}\Phi\mathbf{G}\mathbf{x}(t) + \mathbf{A}\Phi\mathbf{z}(t)\|^2 = (L(d_1) \mathbf{e}^T(\theta_1, M_t) \mathbf{R}_x \mathbf{e}^*(\theta_1, M_t) + \sigma_z^2) \sum_{n=1}^N a_n^2 \leq P_A$. Accordingly, the received echo signals by the active IRS under hypotheses \mathcal{H}_0 and \mathcal{H}_1 at symbol $t \in \mathcal{T}$ are respectively given by

$$\begin{cases} \mathcal{H}_0 : & \mathbf{y}(t) = \mathbf{n}(t), \\ \mathcal{H}_1 : & \mathbf{y}(t) = \alpha \mathbf{e}(\theta_0, M_r) \mathbf{e}^T(\theta_0, N) \mathbf{A}\Phi\mathbf{G}\mathbf{x}(t) \\ & + \alpha \mathbf{e}(\theta_0, M_r) \mathbf{e}^T(\theta_0, N) \mathbf{A}\Phi\mathbf{z}(t) + \mathbf{n}(t), \end{cases} \quad (1)$$

where $\mathbf{n}(t) \in \mathbb{C}^{M_r \times 1} \sim \mathcal{CN}(\mathbf{0}, \sigma^2 \mathbf{I}_{M_r})$ is the noise at the IRS sensors with σ^2 being the noise power at each IRS’s sensor. Furthermore, we stack the received each signal by the active IRS, the transmitted signal by the BS, the active IRS’s reflection noise, and noise at the IRS’s receiver over the T symbols as $\tilde{\mathbf{y}} = [\mathbf{y}^T(1), \dots, \mathbf{y}^T(T)]^T$, $\tilde{\mathbf{x}} = [\mathbf{x}^T(1), \dots, \mathbf{x}^T(T)]^T$, $\tilde{\mathbf{z}} = [\mathbf{z}^T(1), \dots, \mathbf{z}^T(T)]^T$, and $\tilde{\mathbf{n}} = [\mathbf{n}^T(1), \dots, \mathbf{n}^T(T)]^T$, respectively. Then, the received echo signals at the active IRS under hypotheses \mathcal{H}_0 and \mathcal{H}_1 over the T symbols are respectively given by

$$\begin{cases} \mathcal{H}_0 : & \tilde{\mathbf{y}} = \tilde{\mathbf{n}}, \\ \mathcal{H}_1 : & \tilde{\mathbf{y}} = (\mathbf{I}_T \otimes \alpha \mathbf{e}(\theta_0, M_r) \mathbf{e}^T(\theta_0, N) \mathbf{A}\Phi\mathbf{G}) \tilde{\mathbf{x}} \\ & + (\mathbf{I}_T \otimes \alpha \mathbf{e}(\theta_0, M_r) \mathbf{e}^T(\theta_0, N) \mathbf{A}\Phi) \tilde{\mathbf{z}} + \tilde{\mathbf{n}}. \end{cases} \quad (2)$$

Based on the received echo signals in (2), we aim to detect the presence of the target. The difference of received signals between hypotheses \mathcal{H}_0 and \mathcal{H}_1 consists the deterministic component signal $\mathbf{u}_1 = (\mathbf{I}_T \otimes \alpha \mathbf{e}(\theta_0, M_r) \mathbf{e}^T(\theta_0, N) \mathbf{A}\Phi\mathbf{G}) \tilde{\mathbf{x}}$, which is induced by the BS’s transmit signal, and random component signal $\mathbf{u}_2 = (\mathbf{I}_T \otimes \alpha \mathbf{e}(\theta_0, M_r) \mathbf{e}^T(\theta_0, N) \mathbf{A}\Phi) \tilde{\mathbf{z}}$, which is induced by the IRS’s reflection noise. It is thus essential to jointly leverage both deterministic and random signals to fully exploit the available signal dimensions for effective sensing, highlighting the pressing need to optimize transmit and reflective beamforming for enhancing the sensing performance.

III. OPTIMAL TARGET DETECTOR

In this section, we first obtain the optimal detector based on (2) via the NP theorem [18] and then derive the target detection probability under given false alarm probability.

We denote the covariance matrix of the random signal \mathbf{u}_2 as $\mathbf{C} = \mathbb{E}(\mathbf{u}_2 \mathbf{u}_2^H) = \mathbf{I}_T \otimes \sigma_z^2 |\alpha|^2 \sum_{n=1}^N a_n^2 \mathbf{e}(\theta_0, M_r) \mathbf{e}^H(\theta_0, M_r)$. Then, the probability density functions (PDFs) of the received signal $\tilde{\mathbf{y}}$ under hypotheses \mathcal{H}_0 and \mathcal{H}_1 are given as $p(\tilde{\mathbf{y}}; \mathcal{H}_0) = \frac{\exp(-\frac{1}{\sigma^2} \tilde{\mathbf{y}}^H \tilde{\mathbf{y}})}{\pi^{M_r T} \det(\sigma^2 \mathbf{I}_{M_r T})}$ and $p(\tilde{\mathbf{y}}; \mathcal{H}_1) = \frac{\exp(-(\tilde{\mathbf{y}} - \mathbf{u}_1)^H (\mathbf{C} + \sigma^2 \mathbf{I}_{M_r T})^{-1} (\tilde{\mathbf{y}} - \mathbf{u}_1))}{\pi^{M_r T} \det(\mathbf{C} + \sigma^2 \mathbf{I}_{M_r T})}$, respectively. For the binary detection task, we adopt the NP theorem to establish the optimal detection rule [18], which aims to determine the optimal decision threshold to maximize the detection probability under a predetermined false alarm probability.

The NP detector is $\frac{p(\tilde{\mathbf{y}}; \mathcal{H}_1)}{p(\tilde{\mathbf{y}}; \mathcal{H}_0)} \stackrel{\mathcal{H}_1}{\gtrless} \delta$, which is equivalent to $\ln \frac{p(\tilde{\mathbf{y}}; \mathcal{H}_1)}{p(\tilde{\mathbf{y}}; \mathcal{H}_0)} = \tilde{\mathbf{y}}^H \frac{1}{\sigma^2} \mathbf{C} (\mathbf{C} + \sigma^2 \mathbf{I}_{M_r T})^{-1} \tilde{\mathbf{y}} - \mathbf{u}_1^H (\mathbf{C} + \sigma^2 \mathbf{I}_{M_r T})^{-1} \mathbf{u}_1 + 2\text{Re} \{ \mathbf{u}_1^H (\mathbf{C} + \sigma^2 \mathbf{I}_{M_r T})^{-1} \tilde{\mathbf{y}} \} + M_r T \ln \sigma^2 - \ln \det(\mathbf{C} + \sigma^2 \mathbf{I}_{M_r T}) \stackrel{\mathcal{H}_1}{\gtrless} \ln \delta$, where the detection threshold δ is determined with the given false alarm probability P_{FA} ³. By letting $\delta' = \ln \delta + \mathbf{u}_1^H (\mathbf{C} + \sigma^2 \mathbf{I}_{M_r T})^{-1} \mathbf{u}_1 - M_r T \ln \sigma^2 + \ln \det(\mathbf{C} + \sigma^2 \mathbf{I}_{M_r T})$, we obtain the optimal detector as $T(\tilde{\mathbf{y}}) = \tilde{\mathbf{y}}^H \frac{1}{\sigma^2} \mathbf{C} (\mathbf{C} + \sigma^2 \mathbf{I}_{M_r T})^{-1} \tilde{\mathbf{y}} + 2\text{Re} \{ \mathbf{u}_1^H (\mathbf{C} + \sigma^2 \mathbf{I}_{M_r T})^{-1} \tilde{\mathbf{y}} \} \stackrel{\mathcal{H}_1}{\gtrless} \delta'$.

Remark 1: For the optimal detector $T(\tilde{\mathbf{y}})$, both the BS's transmit signal $\mathbf{x}(t)$ and IRS's reflection noise $\mathbf{z}(t)$ are effectively utilized for detection. Therefore, it is expected that the IRS's reflection noise can be harnessed to enhance the detection performance, as will be shown in Section V.

Then, we have the following proposition to analyze the detection performance.

Proposition 1: The detection probability $P_D(\mathbf{R}_x, \Phi, \mathbf{A})$ under a predetermined false alarm probability P_{FA} is

$$P_D(\mathbf{R}_x, \Phi, \mathbf{A}) = \mathcal{Q}_{\chi_{2T}^2(\lambda_2)} \left(\frac{\mathcal{Q}_{\chi_{2T}^2(\lambda_1)}^{-1}(P_{FA})}{1 + |\alpha|^2 M_r \sum_{n=1}^N a_n^2 \sigma_z^2 / \sigma^2} \right), \quad (3)$$

with $\lambda_1 = \frac{2\sigma^2 T \mathbf{e}^T(\theta_0, N) \mathbf{A} \Phi \mathbf{G} \mathbf{R}_x \mathbf{G}^H \Phi^H \mathbf{A}^H \mathbf{e}^*(\theta_0, N)}{(\sum_{n=1}^N a_n^2)^2 M_r \sigma_d^4 |\alpha|^2}$ and $\lambda_2 = \lambda_1 (1 + |\alpha|^2 \sum_{n=1}^N a_n^2 M_r \sigma_z^2 / \sigma^2)$ being the non-centrality parameters of non-central chi-squared distributions.

Proof: Please refer to Appendix A. \blacksquare

Proposition 1 reveals the achieved detection probability, which, however, is a highly non-convex and non-explicit function due to the right-tail function of non-central chi-squared distributions in (3). As such, it is difficult to adopt $P_D(\mathbf{R}_x, \Phi, \mathbf{A})$ as the objective function directly for optimizing the joint beamforming. To tackle this issue, we further approximate the detection probability by considering the special asymptotical case when the number of symbols T is sufficiently large.

Proposition 2: When T becomes sufficiently large, the detection probability in (3) approaches (4) as given at the top of next page.

³The closed-form relation between δ and P_{FA} is derived in Appendix A.

Proof: According to the central limit theorem, the PDF of chi-squared distribution becomes Gaussian when the degrees of freedom, $2T$, are sufficiently large [18]. Thus, the detection probability in (3) is approximated as (4). The detailed proof is given in Appendix B. \blacksquare

We have the following interesting observation based on Proposition 2.

Proposition 3: Given fixed IRS amplification matrix \mathbf{A} , the detection probability $\tilde{P}_D(\mathbf{R}_x, \Phi, \mathbf{A})$ is monotonically increasing w.r.t. the non-centrality parameter λ_1 .

Proof: This lemma follows directly by calculating the derivation of $\tilde{P}_D(\mathbf{R}_x, \Phi, \mathbf{A})$ w.r.t. λ_1 , which is larger than zero. \blacksquare

IV. TARGET DETECTION PROBABILITY MAXIMIZATION VIA JOINT BEAMFORMING

In this section, we aim to maximize the detection probability by jointly optimizing the transmit beamforming at the BS, as well as the phase shift and amplification matrices at the active IRS. By exploiting the approximate detection probability in (4) as the objective function, the detection probability maximization problem is formulated as

$$(P1) : \max_{\mathbf{R}_x \succeq 0, \Phi, \mathbf{A}} \tilde{P}_D(\mathbf{R}_x, \Phi, \mathbf{A})$$

$$\text{s.t. } |\Phi_{n,n}| = 1, \forall n \in \mathcal{N}, \quad (5a)$$

$$0 \leq a_n \leq a_{\max}, \forall n \in \mathcal{N}, \quad (5b)$$

$$(L(d_1) \mathbf{e}^T(\theta_1, M_t) \mathbf{R}_x \mathbf{e}^*(\theta_1, M_t) + \sigma_z^2) \sum_{n=1}^N a_n^2 \leq P_A, \quad (5c)$$

$$\text{tr}(\mathbf{R}_x) \leq P. \quad (5d)$$

In the following, we adopt nested optimization to solve problem (P1) optimally. First, we derive optimal \mathbf{R}_x and Φ in a closed form under any given \mathbf{A} . Based on Proposition 3, maximizing $\tilde{P}_D(\mathbf{R}_x, \Phi, \mathbf{A})$ is equivalent to maximizing λ_1 under given \mathbf{A} . Therefore, the optimization of \mathbf{R} and Φ is formulated as

$$(P2) : \max_{\mathbf{R}_x \succeq 0, \Phi} \mathbf{e}^T(\theta_0, N) \mathbf{A} \Phi \mathbf{G} \mathbf{R}_x \mathbf{G}^H \Phi^H \mathbf{A}^H \mathbf{e}^*(\theta_0, N)$$

$$\text{s.t. } (5a), (5c), \text{ and } (5d).$$

Proposition 4: The optimal solution to problem (P2) is $\mathbf{R}_x^*(\mathbf{A}) = \frac{P_x}{M_t} \mathbf{e}^*(\theta_1, M_t) \mathbf{e}^T(\theta_1, M_t)$ with $P_x = \min \{ P, (P_A / \sum_{n=1}^N a_n^2 - \sigma_z^2) / (L(d_1) M_t) \}$ and $\Phi^* = \text{diag}(e^{j\phi_1^*}, \dots, e^{j\phi_N^*})$ with $\phi_n^* = -j2\pi(n-1)d_2(\sin \theta_0 + \sin \theta_2) / \lambda, \forall n \in \mathcal{N}$.

Proof: The optimal transmit beamforming at the BS is obtained based on the maximum ratio transmission. Besides, the optimal reflecting phase shift design is achieved by aligning the multi-path signals toward the sensing target. \blacksquare

Next, we substitute the obtained $\mathbf{R}_x^*(\mathbf{A})$ and Φ^* back to problem (P1) and then optimize \mathbf{A} , which is formulated as

$$(P3) : \max_{\mathbf{A}, P_x} \tilde{P}_D(\mathbf{R}_x^*(\mathbf{A}), \Phi^*, \mathbf{A})$$

$$\text{s.t. } 0 \leq a_n \leq a_{\max}, \forall n \in \mathcal{N}, \quad (6a)$$

$$(L(d_1) M_t P_x + \sigma_z^2) \sum_{n=1}^N a_n^2 \leq P_A, \quad (6b)$$

$$0 \leq P_x \leq P. \quad (6c)$$

$$\tilde{P}_D(\mathbf{R}_x, \Phi, \mathbf{A}) = \mathcal{Q} \left(\frac{\sqrt{T + \lambda_1} \mathcal{Q}^{-1} \left(\tilde{P}_{FA} \right) - |\alpha|^2 M_r \sum_{n=1}^N a_n^2 T \sigma_z^2 / \sigma^2 - \lambda_1 \left((1 + |\alpha|^2 M_r \sum_{n=1}^N a_n^2 \sigma_z^2 / \sigma^2)^2 - 1 \right) / 2}{\left(1 + |\alpha|^2 M_r \sum_{n=1}^N a_n^2 \sigma_z^2 / \sigma^2 \right) \sqrt{T + \lambda_1 \left(1 + |\alpha|^2 M_r \sum_{n=1}^N a_n^2 \sigma_z^2 / \sigma^2 \right)}} \right). \quad (4)$$

We have the following proposition for revealing problem (P3).

Proposition 5: The optimality of problem (P3) is attained when $a_n = a_0, \forall n \in \mathcal{N}$.

Proof: With the optimal \mathbf{R}_x^* and Φ^* , we have $\lambda_1 = \frac{2\sigma^2 TL(d) M_t P_x (\sum_{n=1}^N a_n)^2}{(\sum_{n=1}^N a_n^2)^2 M_r \sigma_d^4 |\alpha|^2}$. For variable λ_1 , with any given amplification matrix \mathbf{A} , we all have $(\sum_{n=1}^N a_n)^2 \leq N \sum_{n=1}^N a_n^2$, where the inequality holds if and only if $a_n = a_0, \forall n \in \mathcal{N}$. Then, as the detection probability $P_D(\mathbf{R}_x, \Phi, \mathbf{A})$ increases monotonically w.r.t. λ_1 , Proposition 5 is obtained. ■

As variable λ_1 is monotonically increasing w.r.t. P_x , based on Proposition 3, the optimality of problem (P3) is attained when at least one of the constraints (6b) and (6c) is tight. Then, applying Proposition 5, problem (P3) can be optimally solved by a one-dimensional search of the feasible region of variable a_0 . Therefore, problem (P1) is optimally solved.

V. NUMERICAL RESULTS

In this section, we present simulation results to verify the detection performance of our proposed detector and beamforming design. We set the numbers of transmit antennas at the BS and the receive sensors at the active IRS as $M_t = M_r = 8$. The distance-dependent path loss at distance d is modeled as $L(d) = K_0(d/d_0)^{-\beta}$ with $K_0 = -30$ dB being the path loss at the reference distance $d_0 = 1$ m and $\beta = 2.2$. The distances of the BS-IRS and IRS-target links are set as $d_1 = 120$ m and $d_2 = 10$ m, respectively. The target's RCS is set as $\beta = 1$. The false alarm probability is set as $\tilde{P}_{FA} = 10^{-3}$. We also set $\theta_0 = \theta_1 = \theta_2 = \pi/4$, $P = 30$ dBm, $P_A = 15$ dBm, $\sigma^2 = -70$ dBm, and $\sigma_z^2 = -30$ dBm. For comparison, we also consider the following benchmark schemes, as well as the fully- and semi-passive IRS-enabled target detection [7] with the maximum transmit power at the BS being $P + P_A$.

1) *Sensing signal-to-noise ratio (SNR)-based detector:* In this benchmark scheme, the detector is designed based on the received sensing SNR $\gamma = \frac{|\alpha|^2 \mathbf{e}^T(\theta_0, N) \mathbf{A} \Phi \mathbf{G} \mathbf{R}_x \mathbf{G}^H \Phi^H \mathbf{A}^H \mathbf{e}^*(\theta_0, N)}{|\alpha|^2 \mathbf{e}^T(\theta_0, N) \mathbf{A} \Phi \mathbf{G}^H \mathbf{A}^H \mathbf{e}^*(\theta_0, N) \sigma_z^2 + \sigma^2}$. This approach is based on that in semi-passive IRS-enabled target detection [7]. Accordingly, the joint beamforming is optimized to maximize the sensing SNR γ .

2) *Reflective beamforming only:* We leverage the proposed detector in Section III and only optimize the amplification and reflecting phase shift matrices at the IRS with the sample covariance matrix $\mathbf{R}_x = P/M_t \mathbf{I}_{M_t}$, to maximize the target detection probability in (4).

3) *Transmit beamforming only:* We adopt the proposed detector in Section III and only optimize the transmit beamforming at the BS with the maximum IRS amplification matrix $\mathbf{A} = \text{diag}(a'_\text{max}, \dots, a'_\text{max})$, $a'_\text{max} = \min(a_\text{max}, \sqrt{P_A/(N\sigma_z^2)})$ and adopt a random phase shift matrix, to maximize the target detection probability in (4).

Figs. 2 and 3 illustrate the detection probabilities versus the number of sensing symbols T and the number of reflecting elements N , respectively.

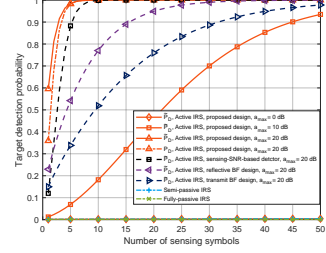


Fig. 2. The detection probability versus the number of sensing symbols T , where $N = 16$.

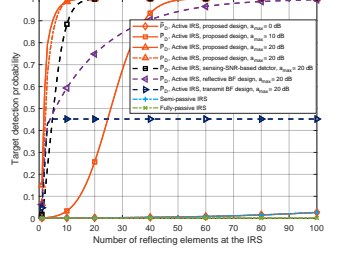


Fig. 3. The detection probability versus the number of reflecting elements N , where $T = 8$.

elements N at the active IRS, respectively. It is demonstrated that the detection probability $P_D(\mathbf{R}_x, \Phi, \mathbf{A})$ in (3) closely approximates as $\tilde{P}_D(\mathbf{R}_x, \Phi, \mathbf{A})$ in (4) when the the number of sensing symbols $T \geq 5$, thus verifying the accuracy of our approximation. It is also shown that our proposed joint beamforming design outperforms the benchmark adopting the sensing-SNR-based detector. This superiority stems from our design's ability to exploit both the BS's transmit signal and the active IRS's reflection noise, while the sensing-SNR-based detector only utilizes the BS's transmit signal and treats the active IRS's reflection noise as harmful interference. Meanwhile, it is also observed that our proposed design with active IRS achieves significantly higher detection probability than the counterparts with semi-passive and fully-passive IRSs. The results show the advantages of signal amplification at the active IRS. Furthermore, it is observed that our proposed joint beamforming design achieves enhanced sensing performance as compared to the benchmark schemes with only reflective or transmit beamforming. This validates the effectiveness of joint beamforming in enhancing detection performance.

VI. CONCLUSION

This letter studied the active IRS-enabled target detection, with the objective of detecting the presence of a target by processing echo signals through the BS-IRS-target-IRS link. Utilizing the NP theorem, we designed an optimal detector by jointly leveraging the BS's transmit signal and the active IRS's reflection noise. After that, we jointly optimized the transmit and reflective beamforming to maximize the detection probability. Simulation results demonstrated that signal amplification at the active IRS, the utilization of the IRS's reflection noise for detector design, and the joint beamforming optimization can significantly increase detection probability.

APPENDIX

A. Proof of Proposition 1

First, we consider the case when the target is absent. In this case, the detector $T(\tilde{\mathbf{y}})$ becomes $T(\tilde{\mathbf{y}}; \mathcal{H}_0) = -\sum_{t=1}^T \left| \frac{(1-k_1 M_r) \alpha \mathbf{e}^T(\theta_0, N) \mathbf{A} \Phi \mathbf{G} \mathbf{x}(t)}{\sigma \sqrt{k_1}} \right|^2 + \sum_{t=1}^T \left| \frac{\sqrt{k_1}}{\sigma} \mathbf{e}^H(\theta_0, M_r) \mathbf{n}(t) + \frac{(1-k_1 M_r)}{\sigma \sqrt{k_1}} \alpha \mathbf{e}^T(\theta_0, N) \mathbf{A} \Phi \mathbf{G} \mathbf{x}(t) \right|^2$

$$\tilde{P}_D = \mathcal{Q} \left(\frac{\frac{2}{k_1(M_r + |\alpha|^2 M_r^2 \sum_{n=1}^N a_n^2 \sigma_z^2 / \sigma^2)} \delta' + \frac{\lambda_1}{1 + |\alpha|^2 M_r \sum_{n=1}^N a_n^2 \sigma_z^2 / \sigma^2} - \lambda_1 \left(1 + |\alpha|^2 \sum_{n=1}^N a_n^2 M_r \sigma_z^2 / \sigma^2 \right) - 2T}{\sqrt{4T + 4\lambda_2}} \right). \quad (9)$$

with $k_1 = \frac{|\alpha|^2 \sum_{n=1}^N a_n^2}{\sigma^2 / \sigma_z^2 + |\alpha|^2 M_r \sum_{n=1}^N a_n^2}$. Due to the fact that $\mathbf{e}^H(\theta_0, M_r) \mathbf{n}(t) \sim \mathcal{CN}(\mathbf{0}, M_r \sigma^2)$, by letting $\mathcal{P}(\theta_0) = \mathbf{e}^T(\theta_0, N) \mathbf{A} \Phi \mathbf{G} \mathbf{R}_x \mathbf{G}^H \Phi^H \mathbf{A}^H \mathbf{e}^*(\theta_0, N)$, we construct an equivalent detector of $T(\tilde{\mathbf{y}}; \mathcal{H}_0)$ as $T'(\tilde{\mathbf{y}}; \mathcal{H}_0) = \frac{T(\tilde{\mathbf{y}}; \mathcal{H}_0) + \frac{(1-k_1 M_r)^2 |\alpha|^2 T \mathcal{P}(\theta_0)}{\sigma^2 k_1}}{k_1 M_r / 2}$, which is the sum squares of independent and identically distribution (i.i.d.) Gaussian random vectors with mean values $\sqrt{\frac{2}{M_r}} \frac{(1-k_1 M_r)}{\sigma k_1} \alpha \mathbf{e}^T(\theta_0, N) \mathbf{A} \Phi \mathbf{G} \mathbf{x}(t), t \in \mathcal{T}$ and variance 1, and thus follows non-central chi-squared distribution with PDF

$$p_1(x) = \begin{cases} \frac{1}{2} \left(\frac{x}{\lambda} \right)^{\frac{\nu_1-2}{4}} \exp \left[-\frac{1}{2}(x+\lambda_1) \right] I_{\frac{\nu_1}{2}-1}(\sqrt{\lambda_1 x}), & x > 0, \\ 0, & x < 0, \end{cases} \quad (7)$$

where the degrees of freedom are $\nu_1 = 2T$, the non-centrality parameter is $\lambda_1 = \frac{2\sigma^2 T \mathcal{P}(\theta_0)}{(\sum_{n=1}^N a_n^2)^2 M_r \sigma_d^4 |\alpha|^2}$, and $I_r(u)$ is the modified Bessel function of the first kind and order r . Accordingly, the false alarm probability P_{FA} given threshold δ' is given as $P_{FA} = \mathcal{Q}_{\chi_{2T}^2(\lambda_1)} \left(\frac{2}{k_1 M_r} \delta' + \lambda_1 \right)$, where $\mathcal{Q}_{\chi_{2T}^2(\lambda_1)}(x) = \int_x^\infty p_1(x) dx, x > 0$.

Next, we consider the case when the target is present and derive the detection probability. In this case, the detector $T(\tilde{\mathbf{y}})$ becomes

$$T(\tilde{\mathbf{y}}; \mathcal{H}_1) = - \sum_{t=1}^T \left| \frac{(1-k_1 M_r) \alpha \mathbf{e}^T(\theta_0, N) \mathbf{A} \Phi \mathbf{G} \mathbf{x}(t)}{\sigma \sqrt{k_1}} \right|^2 + \sum_{t=1}^T \left| \frac{\sqrt{k_1}}{\sigma} \mathbf{e}^H(\theta_0, M_r) \mathbf{y}(t) \frac{(1-k_1 M_r)}{\sigma \sqrt{k_1}} \alpha \mathbf{e}^T(\theta_0, N) \mathbf{A} \Phi \mathbf{G} \mathbf{x}(t) \right|^2.$$

As $\mathbf{e}^H(\theta_0, M_r) \mathbf{y}(t) \sim \mathcal{CN}(\alpha M_r \mathbf{e}^T(\theta_0, M_r) \mathbf{A} \Phi \mathbf{G} \mathbf{x}(t), M_r \sigma^2 + |\alpha|^2 M_r^2 \sum_{n=1}^N a_n^2 \sigma_z^2)$, we construct an equivalent detector of $T(\mathbf{y}; \mathcal{H}_1)$ as $T'(\tilde{\mathbf{y}}; \mathcal{H}_1) = \frac{T(\mathbf{y}; \mathcal{H}_1) + \frac{(1-k_1 M_r)^2 |\alpha|^2 T \mathcal{P}(\theta_0)}{\sigma^2 k_1}}{k_1 (M_r + |\alpha|^2 M_r^2 \sum_{n=1}^N a_n^2 \sigma_z^2 / \sigma^2) / 2}$, which follows non-central chi-squared distribution with PDF

$$p_2(x) = \begin{cases} \frac{1}{2} \left(\frac{x}{\lambda} \right)^{\frac{\nu_2-2}{4}} \exp \left[-\frac{1}{2}(x+\lambda_2) \right] I_{\frac{\nu_2}{2}-1}(\sqrt{\lambda_2 x}), & x > 0, \\ 0, & x < 0, \end{cases} \quad (8)$$

where the degrees of freedom are $\nu_2 = 2T$ and the non-centrality parameter is $\lambda_2 = \lambda_1 (1 + |\alpha|^2 \sum_{n=1}^N a_n^2 M_r \sigma_z^2 / \sigma^2)$. Accordingly, the detection probability P_D given threshold δ' is given as $P_D = \mathcal{Q}_{\chi_{2T}^2(\lambda_2)} \left(\frac{2}{k_1 (M_r + |\alpha|^2 M_r^2 \sum_{n=1}^N a_n^2 \sigma_z^2 / \sigma^2)} \delta' + \lambda_1 \left(1 + |\alpha|^2 \sum_{n=1}^N a_n^2 M_r \sigma_z^2 / \sigma^2 \right) \right)$, where $\mathcal{Q}_{\chi_{2T}^2(\lambda_2)}(x) = \int_x^\infty p_2(x) dx, x > 0$. Finally, we obtain the detection probability under given false alarm probability in (3).

B. Proof of Proposition 2

When T is sufficiently large, the central limit theorem implies that the distributions of $T'(\tilde{\mathbf{y}}; \mathcal{H}_0)$ and $T'(\tilde{\mathbf{y}}; \mathcal{H}_1)$ approach Gaussian [18], i.e., $T'(\tilde{\mathbf{y}}; \mathcal{H}_0) \approx T''(\tilde{\mathbf{y}}; \mathcal{H}_0) \sim \mathcal{N}(\nu_1 + \lambda_1, 2\nu_1 + 4\lambda_1)$ and $T'(\tilde{\mathbf{y}}; \mathcal{H}_1) \approx T''(\tilde{\mathbf{y}}; \mathcal{H}_1) \sim \mathcal{N}(\nu_2 + \lambda_2, 2\nu_2 + 4\lambda_2)$. Accordingly, the false alarm probability P_{FA} and detection probability P_D becomes $\tilde{P}_{FA} =$

$\mathcal{Q} \left(\frac{\frac{2}{k_1 M_r} \delta' - 2T}{\sqrt{4T + 4\lambda_1}} \right)$ and \tilde{P}_D in (9) as given at the top of this page. Based on these, the detection probability under a predetermined false alarm probability is given in (4).

REFERENCES

- [1] X. Shao, C. You, and R. Zhang, "Intelligent reflecting surface aided wireless sensing: Applications and design issues," *IEEE Wireless Commun.*, vol. 31, no. 3, pp. 383–389, Jun. 2024.
- [2] R. Liu, M. Li, H. Luo, Q. Liu, and A. L. Swindlehurst, "Integrated sensing and communication with reconfigurable intelligent surfaces: Opportunities, applications, and future directions," *IEEE Wireless Commun.*, vol. 30, no. 1, pp. 50–57, Feb. 2023.
- [3] S. P. Chepuri, N. Shlezinger, F. Liu, G. C. Alexandropoulos, S. Buzzi, and Y. C. Eldar, "Integrated sensing and communications with reconfigurable intelligent surfaces: From signal modeling to processing," *IEEE Signal Process. Mag.*, vol. 40, no. 6, pp. 41–62, Sep. 2023.
- [4] X. Song, J. Xu, F. Liu, T. X. Han, and Y. C. Eldar, "Intelligent reflecting surface enabled sensing: Cramér-Rao bound optimization," *IEEE Trans. on Signal Process.*, vol. 71, pp. 2011–2026, May 2023.
- [5] S. Buzzi, E. Grossi, M. Lops, and L. Venturino, "Foundations of MIMO radar detection aided by reconfigurable intelligent surfaces," *IEEE Trans. on Signal Process.*, vol. 70, pp. 1749–1763, Mar. 2022.
- [6] X. Shao, C. You, W. Ma, X. Chen, and R. Zhang, "Target sensing with intelligent reflecting surface: Architecture and performance," *IEEE J. Sel. Areas Commun.*, vol. 40, no. 7, pp. 2070–2084, Jul. 2022.
- [7] X. Song, X. Li, X. Qin, J. Xu, T. X. Han, and D. W. K. Ng, "Fully-passive versus semi-passive IRS-enabled sensing: SNR and CRB comparison," Nov. 2023. [Online]. Available: <https://arxiv.org/pdf/2311.06002.pdf>
- [8] Y. Fang, X. Yu, J. Xu, and Y.-J. A. Zhang, "Multi-active-IRS-assisted cooperative sensing: Cramér-Rao bound and joint beamforming design," Jul. 2024. [Online]. Available: <https://arxiv.org/pdf/2406.12426.pdf>
- [9] J. Li, G. Zhou, T. Gong, and N. Liu, "Beamforming design for active IRS-aided MIMO integrated sensing and communication systems," *IEEE Wireless Commun. Letters*, vol. 12, no. 10, pp. 1786–1790, Oct. 2023.
- [10] Y. Zhang, J. Chen, C. Zhong, H. Peng, and W. Lu, "Active IRS-assisted integrated sensing and communication in C-RAN," *IEEE Wireless Commun. Letters*, vol. 12, no. 3, pp. 411–415, Mar. 2023.
- [11] Q. Zhu, M. Li, R. Liu, and Q. Liu, "Joint transceiver beamforming and reflecting design for active RIS-aided ISAC systems," *IEEE Trans. Veh. Technol.*, vol. 72, no. 7, pp. 9636–9640, Jul. 2023.
- [12] Z. Yu, H. Ren, C. Pan, G. Zhou, B. Wang, M. Dong, and J. Wang, "Active RIS-aided ISAC systems: Beamforming design and performance analysis," *IEEE Trans. on Commun.*, vol. 72, no. 3, pp. 1578–1595, Mar. 2024.
- [13] Q. Zhu, M. Li, R. Liu, and Q. Liu, "Cramér-Rao bound optimization for active RIS-empowered ISAC systems," *IEEE Trans. on Wireless Commun.*, early access, Apr. 2024, doi:10.1109/TWC.2024.3384501.
- [14] Z. Zhang, L. Dai, X. Chen, C. Liu, F. Yang, R. Schober, and H. V. Poor, "Active RIS vs. passive RIS: Which will prevail in 6G?" *IEEE Trans. on Commun.*, vol. 71, no. 3, pp. 1707–1725, Mar. 2023.
- [15] R. Long, Y.-C. Liang, Y. Pei, and E. G. Larsson, "Active reconfigurable intelligent surface-aided wireless communications," *IEEE Trans. on Wireless Commun.*, vol. 20, no. 8, pp. 4962–4975, Aug. 2021.
- [16] M. Fu, W. Mei, and R. Zhang, "Multi-active/passive-IRS enabled wireless information and power transfer: Active IRS deployment and performance analysis," *IEEE Commun. Lett.*, vol. 27, no. 8, pp. 2217–2221, Aug. 2023.
- [17] Z. Kang, C. You, and R. Zhang, "Double-active-IRS aided wireless communication: Deployment optimization and capacity scaling," *IEEE Wireless Commun. Lett.*, vol. 12, no. 11, pp. 1821–1825, Nov. 2023.
- [18] S. M. Kay, *Fundamentals of Statistical Signal Processing Volume II: Detection Theory*. PTR Prentice-Hall, Englewood Cliffs, NJ, 1993.